Eur Spine J (2012) 21:863–871
DOI 10.1007/s00586-011-2085-y

ORIGINAL ARTICLE

Posterior fixation and fusion of unstable Hangman's fracture by using intraoperative three-dimensional fluoroscopy-based navigation

Wei Tian · Chong Weng · Bo Liu · Qin Li · Lin Hu · Zhi-Yu Li · Ya-Jun Liu · Yu-Zhen Sun

Received: 30 June 2011 / Revised: 29 October 2011 / Accepted: 12 November 2011 / Published online: 23 November 2011

Abstract
Purpose The purpose of this study was to assess the efficacy and accuracy of posterior screw fixation for unstable Hangman's fracture using intraoperative 3D fluoroscopy-based navigation.
Methods 14 patients with unstable Hangman's fractures (11 males and 3 females), ranging in age from 21 to 59 years, received posterior fixation assisted by an intraoperative 3D fluoroscopy-based navigation system: 11 Levine–Edwards type II and three type IIA cases. The American Spine Injury Association grade was D in 2 and E in 12 cases.
Results Operation time was 110 min (range 90–140 min). Hospital stay was 7.6 days (range 5–12 days). All the patients were observed for an average of 28.8 months (range 15–50 months). No screw-related injury to nerve, or vertebral artery was observed intraoperatively. An average of four screws/patient were inserted. Pedicle screws were placed into C2 and C3, and 5 screws were into the lateral mass of C3. Screw placement accuracy was evaluated using postoperative CT, according to the modified classification of Gertzbein and Robbins; one screw was grade 2 in C2, and three screws were grade 2 in the pedicle of C3. No grade 3 misplacement or clinical deficits were noted. C3 lateral mass screws were successfully inserted. Neck pain was relieved in each case. Neurologic status improved from D to E in 2 cases. Solid fusion was demonstrated in all the cases by static and dynamic films during the final follow-up.
Conclusions This case series demonstrates that intraoperative 3D fluoroscopy-based navigation is a safe, accurate, and effective tool for screw placement in patients with unstable Hangman's fracture.

Keywords Three-dimensional fluoroscopy · Hangman's fracture · Screw fixation · Intraoperative navigation · Traumatic spondylolisthesis of the axis

W. Tian (✉) · C. Weng · B. Liu · Q. Li · L. Hu · Z.-Y. Li · Y.-J. Liu · Y.-Z. Sun
Department of Spine Surgery, Peking University Fourth Clinical Medical College, Beijing Jishuitan Hospital, NO. 31, Xinjiekou East Street, Xicheng District, Beijing, People's Republic of China
e-mail: orthdanielcw@yahoo.com

Introduction

Hangman's fracture, also known as traumatic spondylolisthesis of the axis, is defined as a fracture involving the lamina, articular facets, pedicles, or pars of the axis vertebra. Variable displacement of C2 on C3 is seen [1]. Hangman's fracture is caused by falling, trauma, and motor vehicle accidents (MVA) [2]. According to the classification by Levine and Edwards [3], fractures with concomitant severe circumferential discoligamentous injuries (type II, type IIA, and type III) are thought to be unstable and require rigid immobilization. Opinions vary regarding the optimal treatment of unstable Hangman's fractures. Some recommend the use of rigid orthosis, while others recommend surgical stabilization. Although various methods have been advocated, the optimum surgical treatment remains controversial [2].

The peculiar anatomy of the upper cervical spine is highly variable. The presence of surrounding neurovascular structures make screw fixation more technically challenging. Using conventional techniques, misplacement of screws is reported in up to 21.6% of such procedures [4]. The advent of intraoperative 3D navigation systems permit

safe and accurate instrumentation of the cervical spine [5]; however, only a few small series are available on its use in Hangman's fracture [6, 7]. The purpose of this study was to evaluate the feasibility and accuracy of installing screws in unstable Hangman's fracture cases by using intraoperative 3D fluoroscopy-based navigation.

Materials and methods

A total of 14 consecutive patients with type II or IIA fracture were surgically treated with posterior fixation from December 2005 to March 2010. Clinical information is shown in Table 1. The group consisted of 11 males and 3 females between 21 and 59 years of age. Their average age was 38.9 years. According to the classification of Levine and Edwards, all the cases in this group were unstable with type II in 11 cases and type IIA in 3 cases. Fractures were acute with the exception of 3 nonunion fractures treated by 3 months of rigid orthosis. The causes of injury were MVA in 10 cases, falling in 2 cases and other trauma accounted for 2. Six had associated facial soft tissue injuries, one had fracture of C3 lateral mass, one fracture of left clavicle, and one had fracture of mandible. All the patients complained of neck and shoulder pain with restricted motion of the cervical spine. The American Spine Injury Association (ASIA) grade was D in 2 cases and E in the other cases. Injury of the C2–C3 disc was seen by MRI imaging in all. Surgeries are carried out in these unstable fractures and/or after rigid orthosis failure.

Preoperative care

Skull traction was performed in all the patients. Considering the type of the individual case, a weight of 2–4 kg at an appropriate angle was applied to stabilize and reduce the fracture. Some degree of reduction was accomplished in all patients without neural deficits.

Surgical technique

The same senior author performed posterior screw fixation in all the cases using intraoperative 3D fluoroscopy-based navigation system (Fig. 1). This system consists of a modified C-arm CT system (Arcadis Orbic 3D; Siemens, Medical Solutions, Erlangen, Germany) and the workstation of

Table 1 Summary of the data of 14 patients who underwent posterior fixation by using intraoperative 3D fluoroscopy-based navigation systems

Case	Age/ gender	Injury	Diagnosis	Placed screws	ASIA pre/post-op	Hosp. stay (days)	FU (months)	Results
1	32/M	MVA	II + fracture of mandible	4 PS of AXIS	E/E	11	50	Union
2	35/M	MVA	II + STITF	4 PS of AXIS	E/E	8	45	Union
3	39/M	MVA	IIA	4 PS of AXIS	E/E	7	43	Union
4	41/M	MVA	II + failure to conserve treatment	4 PS of SUMMIT	E/E	7	41	Union
5	31/F	MVA	II + fracture of left clavicle	4 PS of SUMMIT	E/E	12	35	Union
6	59/M	MVA	II + fracture of left LMS of C3	3 PS of CDH-M6 1 LMS of C3L	E/E	6	28	Union
7	21/M	Falling	IIA + failure to conserve treatment	2 PS of AXON 2 LMS of C3	D/E	10	25	Union
8	41/M	Others	II	4 PS of CDH-M6	E/E	7	25	Union
9	32/F	MVA	II + STITF	2 PS of AXON 2 LMS of C3	E/E	5	23	Union
10	26/F	MVA	II + STITF	4 PS of AXON	E/E	9	21	Union
11	47/M	MVA	II + STITF	4 PS of AXON	E/E	6	18	Union
12	53/M	MVA	II + failure to conserve treatment	4 PS of AXON	E/E	6	17	Union
13	40/M	Falling	II + STITF	4 PS of AXON	E/E	8	17	Union
14	38/M	Others	IIA + STITF	4 PS of AXON	D/E	5	15	Union

MVA motor vehicle accident, *STITF* soft tissue injury in the face, *Others* hit by a heavy falling objects or fall in ice skating, *PS* pedicle screw, *LMS* lateral mass screw, *FU* follow-up, *AXIS* Medtronic Sofamor Danek Memphis, TN; *SUMMIT* fixation system: Deputy, AcroMed, Cleveland, USA); *AXON* system: Synthes, GmbH, Oberdorf, Switzerland

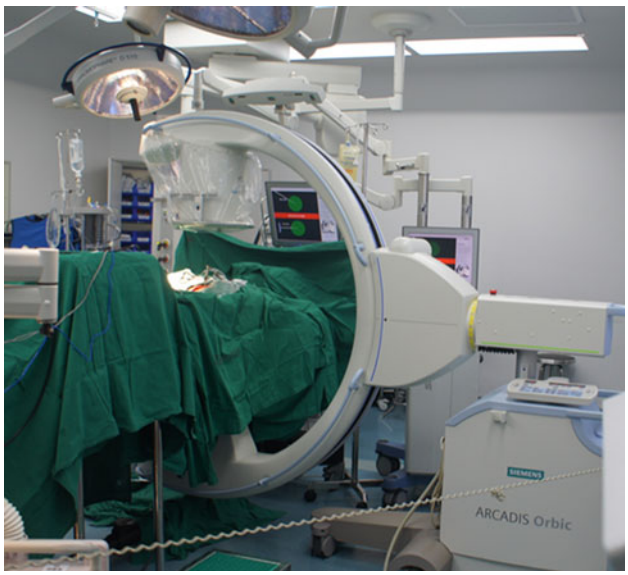

Fig. 1 Operative setup of the intraoperative 3D fluoroscopy-based navigation system with the computer screen facing the surgeon

navigation (The Stryker_ Spine Navigation System, version 1.2, Missouri, USA).

All the patients were operated in a prone position on a radiolucent carbon bed with their heads in a carbon Mayfield head-holder to minimize imaging artifact. Reduction of the fracture dislocation upon positioning was confirmed using intraoperative C-arm images. The normal vertebral line was restored. After the posterior elements of C1–C4 were exposed, the patient tracker was attached to the base of the C4 spinous process. Subsequently, the Arcadis C-arm was positioned, ensuring that the C2–C3 junction was in the center of the fluoroscopic field in the lateral and anterior–posterior (AP) plane. The Arcadis then acquired 100 multiple successive images as it performed an automated 190° rotation around the patient. The acquired images were transferred to the computer navigation workstation to generate axial, sagittal, and coronal reconstruction images and were registered automatically. A tool navigator was used along with the 3D real-time images to determine the entry point, trajectory, length, depth, thickness, and direction of the pedicle and lateral mass screws. The entry point of C2 was prepared using a 2.5-mm high-speed diamond burr that was calibrated to the navigation system so that real-time images could be obtained during drilling. Drilling was applied in stages in order to double-check the accuracy of the trajectory at multiple depths. The operator placed the suitable pedicle screws along the pre-tapped path under the guidance of 3D fluoroscopy-based navigation. C3 pedicle screws were placed subsequently. However, it is difficult to insert C3 pedicle screws effectively in some special situations; for instance, if the C3 pedicle is too small or deformed, or the insertion of C3 pedicle screw conflicts with the patient tracker or the C2 pedicle screw, C3 lateral mass screws were inserted. After instrumentation, the accuracy of the screw placement was again verified by Arcadis-3D. Rods were then connected to the polyaxial screws with locking caps.

Fusion preparation and follow-up

The cartilage surfaces of the C2–C3 articular process were decorticated, and local bone grafts from the spinous process of the C2–C3 were placed in these areas. Patients were out of bed on the second postoperative day with a Philadelphia collar. The duration of immobilization ranged from 2 to 3 months.

Postoperative radiographs and CT images of the cervical spine confirmed that all screws had been placed as planned. Neurological function was assessed 6 months after surgery, and serial radiographs and CT imagines were used to ascertain the fusion status.

Evaluation of the accuracy of pedicle screw implantation

Postoperative CT scans were employed to observe the accuracy of the implanted pedicle screws. The occurrence of complications was based on clinical observations. Using a modified classification of Gertzbein and Robbins, the accuracy of screw placement was classified into 1 of the 3 categories [4, 8, 9]: grade 1 (screw completely within pedicle, Fig. 2a, b); grade2 (<50% of the screw diameter outside the pedicle, Fig. 2c, d); and grade3 (>50% of the screw diameter outside the pedicle).

Results

Postoperative CT scanning revealed satisfactory reduction in all the cases. The average operative time was 110 min (range 90–140 min). Due to the usage of autologous blood transfusion system, none of the patients received blood transfusions. The average time of hospital stay was 7.6 days (range 5–12 days). All the patients were observed for an average of 28.8 months (range 15–50 months). No screw-related injury in the nerves or vertebral artery was observed intraoperatively. No screw revision was necessary. A total of 56 screws were inserted, with 28 pedicle screws with diameter of 3.5 or 4.0 mm placed into C2 pedicle, 23 into the C3 pedicle (3.5 or 4.0 mm), and 5 into the C3 lateral mass (3.5 mm). CT scan, done postoperatively, revealed 1 screw of grade 2 in C2, and 3 screws of grade 2 in C3 pedicle; these grade 2 misplaced screws were

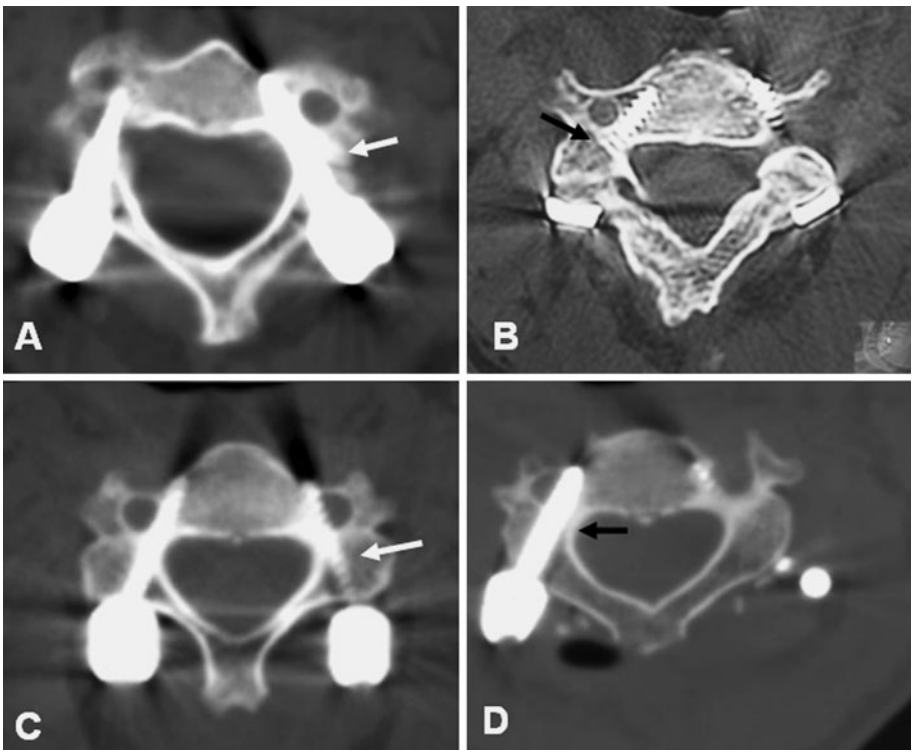

Fig. 2 Grading used for pedicle breaches on postoperative CT scan and the representative postoperative CT scan images: grade 1, no pedicle perforation (**a**, **b**); grade 2, <1/2 diameter of the pedicle screw threads inside the foramen transversarium (**c**, **d**)

clinically silent. A 6-week period of aspirin was suggested to prevent potential thrombosis. There was no grade 3 misplacement and all were without clinical deficits. C3 lateral mass screws were successfully inserted. Neurologic status improved from D to E in all 2 cases. Though there was a subjective report of tension in some patients, the function was not restricted in their daily living. Solid fusion was demonstrated in all the cases by static and dynamic (flexion/extension) films in their final follow-up.

Case presentations

Case 1

A 38-year-old man had severe pain in the neck, with restriction of all neck movements, after being struck by a heavy falling object. He was neurologically intact except for numbness of his left shoulder. CT revealed type II A fracture with large angulation (Fig. 3a, b). MRI showed no cord edema at C2–C3 (Fig. 3c). The fracture reduced well after skull traction with the neck in minimal extension (Fig. 3d). Four cervical pedicle screws were inserted using intraoperative 3D fluoroscopy-based navigation (Fig. 4). After 12 months post-surgery, the patient showed complete recovery from D (preoperatively) to E according to ASIA scale. Good screw placement and solid fusion were noticed (Fig. 5).

Case 2

This patient was a 21-year-old man with severe neck pain following a fall from a height of 3 m. He was noted to have severe muscle spasm with restriction of all neck movements. He had numbness and weakness in both the arms. CT showed the fracture was of type IIA with large angulation (Fig. 6a, b). The fracture failed to unite after 3 months of conservation treatment. When he walked into our department, only numbness in two arms and neck pain were noted. The fracture reduced well after skull traction. Preoperative MRI showed no cord edema and disc herniation at C2–C3 (Fig. 6c). Two pedicle screws in C2 and 2 lateral mass screws in C3 were inserted using intraoperative 3D fluoroscopy-based navigation. After 22 months post-surgery, the patient had complete recovery from D (preoperatively) to E according to the ASIA scale. Postoperative CT and X-ray showed good screw placement and solid fusion (Fig. 7).

Discussion

Hangman's fracture was initially described by Schneider et al. in 1965 [1] and is the most frequent upper cervical fracture after the odontoid fracture. Classification is by the method of Effendi et al. [10] and its modification by Levine and Edwards [3]. Conservative treatment is usually

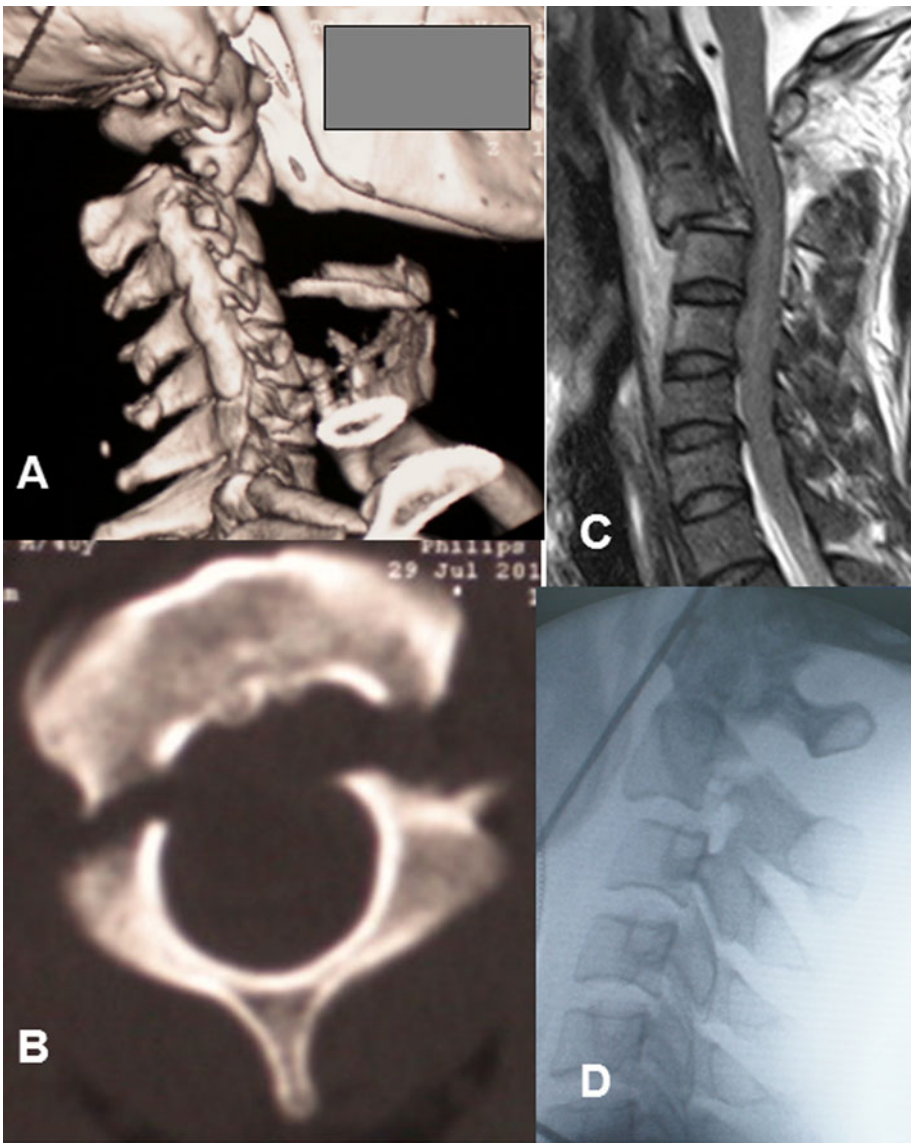

Fig. 3 Type IIA Hangman's fracture: CT reconstruction shows 50% dislocation of C2 relative to C3 with large angulation (**a**), and fractured bilateral pars of the axis (**b**). MRI reveals the severity damaged disc of C2/3 and the compressed spinal canal (**c**). The fracture had reduced well after skull traction before surgery (**d**)

indicated. Union rates for conservative management are 60% in type II, 45% in type IIA, and 35% in type III [2]. The time of immobilization in the Halo or traction device and the possibility of pseudarthrosis, anterior dislocation and kyphosis suggest more aggressive approaches may improve these. The Hangman's fracture is associated with other injuries, which may conflict with rigid immobilization. Considering discoligamentous injury, the dislocation and angulations of fracture, and the desire to shorten recovery, many authors choose surgery for unstable Hangman's fracture [6, 7, 9, 11–13]. Our indications for surgery were unstable fractures (type II, type IIA, and type III) and/or after rigid external orthosis failure.

The ideal fixation system for Hangman's fracture helps to achieve anatomical reduction, a return to painless function, and maintenance of alignment. Several anterior approaches, such as the classical anterior discectomy and fusion techniques (ACDF) and transoral or extraoral approach were applied with C2–C3 discectomy and segmental fixation with bony fusion. ACDF addresses C2–C3 disc herniation and C2–C3 stabilization [11, 14, 15]. Anterior approach, however, does not address the posterior fractured part of the C2. In addition, it may have the disadvantages of approach-related problems; a high anterior approach risks injury to vital structures, especially the facial and hypoglossal nerves, branches of the external carotid artery, contents of the carotid sheath, and the superior laryngeal nerve [16]. The posterior approach, involving a relative simple exposure with no major vascular and visceral structure, can simultaneously fixate the posterior and anterior parts of the C2 vertebra. Among the different posterior approaches, several clinical studies report direct posterior fixation of the pedicles or pars fracture with the advantage of motion reservation in C2–C3

Fig. 4 Accurate entry point and trajectory for pedicle screw insertion into C2 vertebra in the Intraoperative 3D fluoroscopy-based navigation

[6, 17, 18]. However, it is ineffective in patients with unstable fractures due to discoligamentous injury in C2–C3 because it fails to prevent loss of disc height and kyphosis [19]. Redislocations in discoligamentous unstable Hangman's fracture following direct pars repair have been reported [19, 20]. In the biomechanical study by Duggal et al. [21], posterior C2–C3 screw technique was more effective on the stabilization of Hangman's fracture than anterior cervical plating and C2 pars screwing. Our series contains 14 cases of posterior C2–C3 fixation and fusion in types II and IIA Hangman's fracture. This technique not only addresses the detached posterior arch of C2 by repairing the fractured pedicles or pars, but also stabilizes the discoligamentous injury of C2 relative to C3 [13]. A rigid orthosis is also avoided after surgery.

Pedicle screw placement is technically difficult because of the large individual variation in the pedicle dimensions and the course of the vertebral artery. The conventional techniques of screw placement described in the literature rely solely on the external anatomic landmarks to guide screw insertion. Yukawa et al. [4] reported a misplacement rate of grade 2 and grade 3 in 13.1% of 620 cervical pedicle screws using a fluoroscopy-assisted imaging technique. However, the perforation rate in C2 and C3 was 21.6%. This high perforation rate may be partly attributable to the lack of landmarks and an accurate entrance to the cervical pedicles. With the use of continuous radioscopy with a two-dimensional view, potential screw misplacement of C2 and C3 is still present even with experienced hands [13]. Real-time feedback of the proposed screw trajectory in the axial, sagittal, and coronal planes can be achieved by intraoperative 3D navigation [22]. Richter et al. [23] reported excellent results of cervical screw placement using CT-based navigation in a cadaver study. Intraoperative 3D navigation offers a number of advantages [5]. First, motion artifacts are avoided as the images are obtained within the operative room, with the patient in the desired position. This is especially important in unstable situations where preoperative CT scanning may not reflect the actual intraoperative anatomical relationships. Second, the process of manual registration, which includes paired points or surface-matching algorithm, is not required and thus avoids registration errors and improves accuracy. Direct percutaneous screw placement in the axis is possible [7]. Third, all the scanned vertebral levels are auto-registered and make it unnecessary to register at each vertebral level, as is necessary with CT-based navigation. This may also reduce radiation exposure and fluoroscopy time, with advantages for patient and surgeon [24]. Finally, the intraoperative and post-procedural CT images can be acquired by 3D fluoroscopy for verification of the accuracy of the screw placement and cervical alignment [25].

Ito et al. [26] reported a misplacement rate of no more than 2 mm in 2.8% of 176 cervical pedicle screws using Iso-C 3D navigation. In our cases, there were three C3 screw misplacements and only one C2 screw misplacement

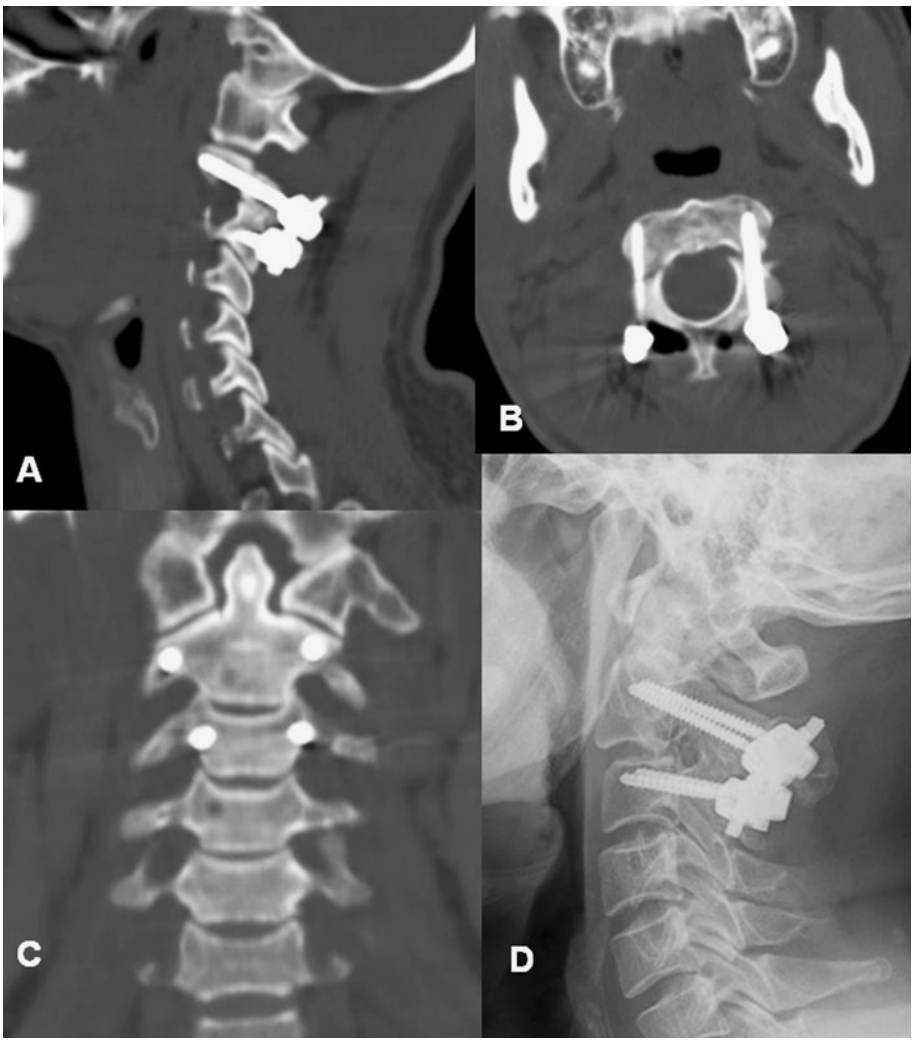

Fig. 5 CT scans made 1 month after surgery, show adequate screw placement in the C2 pedicle, sagittal CT scan (**a**), axial CT scan (**b**), coronal CT scan (**c**). Postoperative lateral roentgenogram 6 months after surgery reveals the normal outline of the C2–C3 and the solid fusion between the articular process of C2–C3

using intraoperative 3D navigation. In our first cases C3 pedicle misplacement was all on the left side. This was thought due to the surgeon's position on the right hand side of the surgery room and vertebral rotation during pedicle screw insertion [27]. Continuous probing to prepare the screw trajectory drilling may perforate the threads inside the foramen transversarium; computed navigation did not allow immediate correction of this. The problem could be avoided by drilling in stages and double-checking the accuracy of the trajectory at multiple depths. The integrity of pre-tapped path was verified with a probe, to ensure that there was no bone breach.

Our clinical results suggest that posterior fixation of Hangman's fracture with screws stabilizes and leads to clinical and radiological union. The hospital stay was relatively short (5–12 days with an average of 7.6 days). Longer hospital stay was due to associated injuries and not related to the surgical procedure. The average operative and hospital stay was comparable to that in case of Hangman's fracture patients from other reports [11–13] (In China, patients get postoperative care as inpatients in the same hospital and are not referred for rehabilitation to another facility [11]). Operation time includes the time of placing patient tracker and getting registration images. Our continuous absorbable suture technique takes more time than staple suture.

The current case series have some limitations. First, it is a small-sized retrospective study and the number of patients was restricted. Second, we did not have a control group for comparison, such as patients undergoing an anterior cervical discectomy and fusion or traditional free-hand technique of posterior polyaxial screw placement. A multicenter prospective controlled study of Hangman's fracture may be considered in the future.

Conclusion

This is the largest series focusing on the usage of intraoperative 3D fluoroscopy-based navigation in unstable Hangman's fracture. This case series demonstrates that

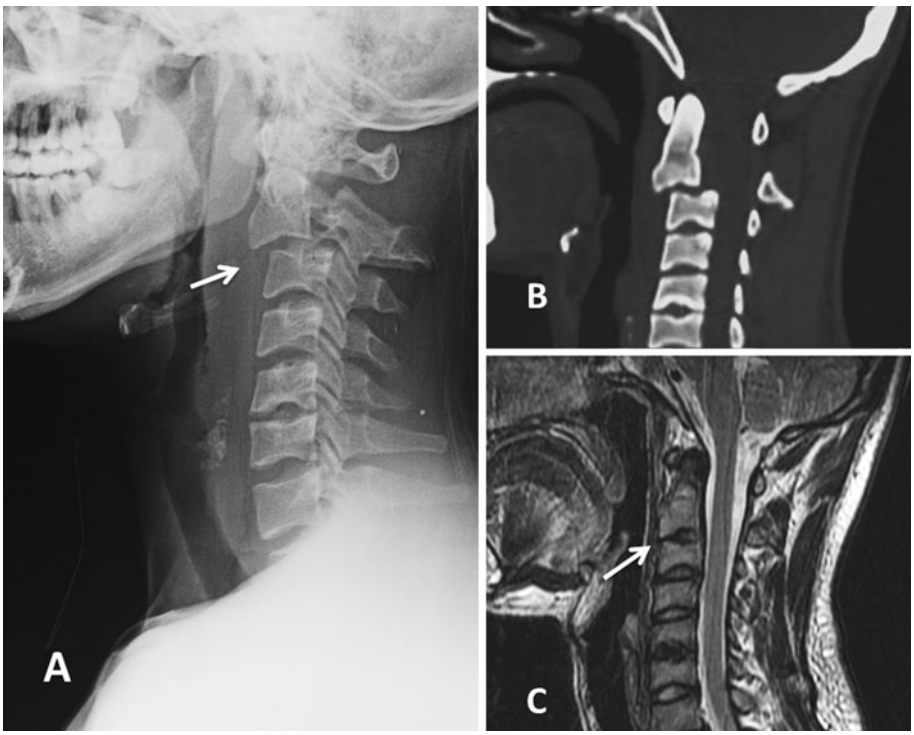

Fig. 6 Preoperative lateral X-ray and CT scan reveals the fracture to be of type IIA with large angulation and hematoma in front of C2–C3 (**a**, **b**). After skull traction, preoperative MRI shows no cord edema and disc herniation at the C2–C3 (**c**)

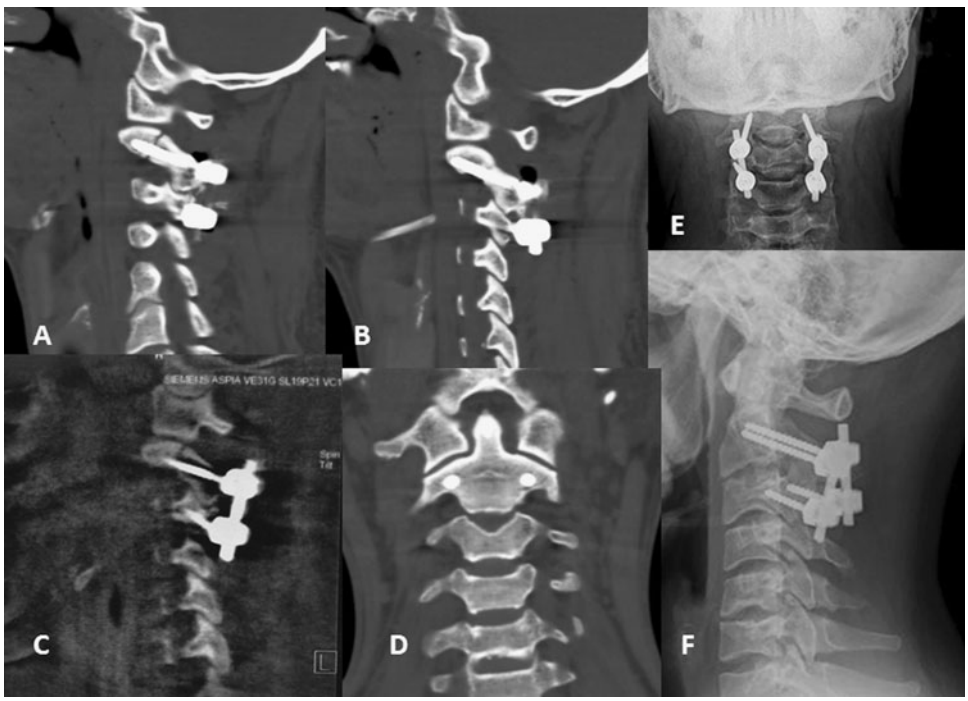

Fig. 7 Postoperative CT scan shows good screw placement in the C2 pedicle, sagittal CT (**a**, **b**) scan, and coronal CT scan (**d**); intraoperative 3D CT scan shows good image quality with clear identification of screw placement (**c**). Postoperative AP and lateral X-ray 6 months after surgery, indicates normal outline of cervical spine and solid fusion between the articular process of the C2–C3 (**e**, **f**)

intraoperative 3D fluoroscopy-based navigation is a safe, accurate, and effective tool for screw placement in patients with unstable Hangman's fracture.

All aspects of this study were approved by our Institutional Review Board and the informed consent was obtained from study participants.

Acknowledgments No funds were received in support of this work. No benefits in any form have been or will be received form a commercial party related directly or indirectly to the subject of this manuscript.

Conflict of interest None.

References

1. Schneider RC, Livingston KE, Cave AJ, Hamilton G (1965) "Hangman's Fracture" of the cervical spine. J Neurosurg 22:141–154. doi:10.3171/jns.1965.22.2.0141
2. Li XF, Dai LY, Lu H, Chen XD (2006) A systematic review of the management of hangman's fractures. Eur Spine J 15:257–269. doi:10.1007/s00586-005-0918-2
3. Levine AM, Edwards CC (1985) The management of traumatic spondylolisthesis of the axis. J Bone Joint Surg Am 67:217–226
4. Yukawa Y, Kato F, Ito K, Horie Y, Hida T, Nakashima H, Machino M (2009) Placement and complications of cervical pedicle screws in 144 cervical trauma patients using pedicle axis view techniques by fluoroscope. Eur Spine J 18:1293–1299. doi:10.1007/s00586-009-1032-7
5. Tjardes T, Shafizadeh S, Rixen D, Paffrath T, Bouillon B, Steinhausen ES, Baethis H (2010) Image-guided spine surgery: state of the art and future directions. Eur Spine J 19:25–45. doi:10.1007/s00586-009-1091-9
6. Rajasekaran S, Vidyadhara S, Shetty AP (2007) Iso-C3D fluoroscopy-based navigation in direct pedicle screw fixation of hangman fracture: a case report. J Spinal Disord Tech 20:616–619. doi:10.1097/BSD.0b013e318074f978
7. Sugimoto Y, Ito Y, Shimokawa T, Shiozaki Y, Mazaki T (2010) Percutaneous screw fixation for traumatic spondylolisthesis of the axis using iso-C3D fluoroscopy-assisted navigation (case report). Minim Invasive Neurosurg 53:83–85. doi:10.1055/s-0030-1247503
8. Gertzbein SD, Robbins SE (1990) Accuracy of pedicular screw placement in vivo. Spine (Phila Pa 1976) 15:11–14
9. Mueller CA, Roesseler L, Podlogar M, Kovacs A, Kristof RA (2010) Accuracy and complications of transpedicular C2 screw placement without the use of spinal navigation. Eur Spine J 19:809–814. doi:10.1007/s00586-010-1291-3
10. Effendi B, Roy D, Cornish B, Dussault RG, Laurin CA (1981) Fractures of the ring of the axis. A classification based on the analysis of 131 cases. J Bone Joint Surg Br 63-B:319–327
11. Ying Z, Wen Y, Xinwei W, Yong T, Hongyu L, Zhu H, Qinggang Z, Weihong Z, Yonggeng C (2008) Anterior cervical discectomy and fusion for unstable traumatic spondylolisthesis of the axis. Spine (Phila Pa 1976) 33:255–258. doi:10.1097/BRS.0b013e31816233d0
12. Xie N, Khoo LT, Yuan W, Ye XJ, Chen DY, Xiao JR, Ni B (2010) Combined anterior C2–C3 fusion and C2 pedicle screw fixation for the treatment of unstable hangman's fracture: a contrast to anterior approach only. Spine (Phila Pa 1976). doi:10.1097/BRS.0b013e3181ba3368
13. Ma W, Xu R, Liu J, Sun S, Zhao L, Hu Y, Jiang W, Liu G, Gu Y (2011) Posterior short-segment fixation and fusion in unstable Hangman's fractures. Spine (Phila Pa 1976) 36:529–533. doi:10.1097/BRS.0b013e3181d60067
14. Tuite GF, Papadopoulos SM, Sonntag VK (1992) Caspar plate fixation for the treatment of complex hangman's fractures. Neurosurgery 30:761–764 (discussion 764–765)
15. Wilson AJ, Marshall RW, Ewart M (1999) Transoral fusion with internal fixation in a displaced hangman's fracture. Spine (Phila Pa 1976) 24:295–298
16. Muller EJ, Wick M, Muhr G (2000) Traumatic spondylolisthesis of the axis: treatment rationale based on the stability of the different fracture types. Eur Spine J 9:123–128
17. Bristol R, Henn JS, Dickman CA (2005) Pars screw fixation of a hangman's fracture: technical case report. Neurosurgery 56:204 (discussion E204)
18. ElMiligui Y, Koptan W, Emran I (2010) Transpedicular screw fixation for type II Hangman's fracture: a motion preserving procedure. Eur Spine J 19:1299–1305. doi:10.1007/s00586-010-1401-2
19. Samaha C, Lazennec JY, Laporte C, Saillant G (2000) Hangman's fracture: the relationship between asymmetry and instability. J Bone Joint Surg Br 82:1046–1052
20. Verheggen R, Jansen J (1998) Hangman's fracture: arguments in favor of surgical therapy for type II and III according to Edwards and Levine. Surg Neurol 49:253–261 (pii:S0090-3019(97)00300-5, discussion 261–262)
21. Duggal N, Chamberlain RH, Perez-Garza LE, Espinoza-Larios A, Sonntag VK, Crawford NR (2007) Hangman's fracture: a biomechanical comparison of stabilization techniques. Spine (Phila Pa 1976) 32:182–187. doi:10.1097/01.brs.0000251917.83529.0b
22. Nottmeier EW, Foy AB (2008) Placement of C2 laminar screws using three-dimensional fluoroscopy-based image guidance. Eur Spine J 17:610–615. doi:10.1007/s00586-007-0557-x
23. Richter M, Amiot LP, Neller S, Kluger P, Puhl W (2000) Computer-assisted surgery in posterior instrumentation of the cervical spine: an in vitro feasibility study. Eur Spine J 9(Suppl 1):65–70
24. Gebhard FT, Kraus MD, Schneider E, Liener UC, Kinzl L, Arand M (2006) Does computer-assisted spine surgery reduce intraoperative radiation doses? Spine (Phila Pa 1976) 31:2024–2027. doi:10.1097/01.brs.0000229250.69369.ac (discussion 2028)
25. Beck M, Mittlmeier T, Gierer P, Harms C, Gradl G (2009) Benefit and accuracy of intraoperative 3D-imaging after pedicle screw placement: a prospective study in stabilizing thoracolumbar fractures. Eur Spine J 18:1469–1477. doi:10.1007/s00586-009-1050-5
26. Ito Y, Sugimoto Y, Tomioka M, Hasegawa Y, Nakago K, Yagata Y (2008) Clinical accuracy of 3D fluoroscopy-assisted cervical pedicle screw insertion. J Neurosurg Spine 9:450–453. doi:10.3171/SPI.2008.9.11.450
27. Sugimoto Y, Ito Y, Tomioka M, Shimokawa T, Shiozaki Y, Mazaki T, Tanaka M (2010) Vertebral rotation during pedicle screw insertion in patients with cervical injury. Acta Neurochir (Wien) 152:1343–1346. doi:10.1007/s00701-010-0665-y